Unsteady Pressure Analysis of a Swirling Flow With Vortex Rope and Axial Water Injection in a Discharge Cone

Article *in* Journal of Fluids Engineering · August 2012

Impact Factor: 0.93 · DOI: 10.1115/1.4007074

4 authors:

Alin Ilie Bosioc
Polytechnic University of Timisoara
47 PUBLICATIONS **181** CITATIONS
SEE PROFILE

Romeo Resiga
Polytechnic University of Timisoara
174 PUBLICATIONS **765** CITATIONS
SEE PROFILE

Sebastian Muntean
Romanian Academy
144 PUBLICATIONS **595** CITATIONS
SEE PROFILE

Constantin Tanasa
Polytechnic University of Timisoara
18 PUBLICATIONS **99** CITATIONS
SEE PROFILE

Alin Ilie Bosioc
Scientific Researcher
Center for Advanced Research
in Engineering Science,
Romanian Academy – Timisoara Branch,
Bvd. Mihai, Viteazu 24,
RO-300223, Timisoara, Romania
e-mail: alin@mh.mec.upt.ro

Romeo Susan-Resiga[1]
Professor
Hydraulic Machinery Department,
"Politehnica" University of Timisoara,
Romania, Bvd. Mihai Viteazu 1,
RO-300222, Timisoara, Romania
e-mail: resiga@mh.mec.upt.ro

Sebastian Muntean
Senior Researcher
Center for Advanced Research
in Engineering Science,
Romanian Academy – Timisoara Branch,
Bvd. Mihai Viteazu 24,
RO-300223, Timisoara, Romania
e-mail: seby@acad-tim.tm.edu.ro

Constantin Tanasa
Research Center for Engineering
of Systems with Complex Fluids,
"Politehnica" University of Timisoara,
Bvd. Mihai Viteazu 1,
RO-300222, Timisoara, Romania
e-mail: costel@mh.mec.upt.ro

Unsteady Pressure Analysis of a Swirling Flow With Vortex Rope and Axial Water Injection in a Discharge Cone

The variable demand of the energy market requires that hydraulic turbines operate at variable conditions, which includes regimes far from the best efficiency point. The vortex rope developed at partial discharges in the conical diffuser is responsible for large pressure pulsations, runner blades breakdowns and may lead to power swing phenomena. A novel method introduced by Resiga et al. (2006, "Jet Control of the Draft Tube in Francis Turbines at Partial Discharge," Proceedings of the 23rd IAHR Symposium on Hydraulic Machinery and Systems, Yokohama, Japan, Paper No. F192) injects an axial water jet from the runner crown downstream in the draft tube cone to mitigate the vortex rope and its consequences. A special test rig was developed at "Politehnica" University of Timisoara in order to investigate different flow control techniques. Consequently, a vortex rope similar to the one developed in a Francis turbine cone at 70% partial discharge is generated in the rig's test section. In order to investigate the new jet control method an auxiliary hydraulic circuit was designed in order to supply the jet. The experimental investigations presented in this paper are concerned with pressure measurements at the wall of the conical diffuser. The pressure fluctuations' Fourier spectra are analyzed in order to assess how the amplitude and dominating frequency are modified by the water injection. It is shown that the water jet injection significantly reduces both the amplitude and the frequency of pressure fluctuations, while improving the pressure recovery in the conical diffuser. [DOI: 10.1115/1.4007074]

Keywords: decelerated swirling flow, vortex rope, water injection method, unsteady pressure, experimental investigation

1 Introduction

The swirling flow emerging from a Francis turbine runner has a major influence in a draft tube cone downstream. It produces self-induced flow instabilities leading to pressure fluctuations and ultimately to the draft tube surge [1]. At part load operation it develops a precessing helical vortex (also known as vortex rope) in the Francis turbine draft tube cone. Consequently, the vortex rope generates pressure fluctuations, additional hydraulic losses, and power swing phenomena at the electrical generator [2]. Unsteady pressure measurements for hydraulic Francis turbines operating at part load have been performed on site by Wang et al. [3] and Baya et al. [4]. They reveal a low frequency oscillation (from 1/5 to 1/3 of the runner rotation frequency) associated with the vortex rope. Extensive unsteady wall pressure measurements in the elbow draft tube of the hydraulic Francis turbine model at partial discharge are performed by Arpe et al. [5]. The pressure waves' source was located near the inner part of the elbow draft tube based on experimental data. Moreover, these waves are propagated in all hydraulic systems. The synchronous nature of the pressure fluctuations and the pressure distribution along the draft tube suggests hydro acoustic resonance of the entire hydraulic system.

Different methods were proposed in order to mitigate the instabilities produced by the vortex rope. Examples include aerators mounted at the inlet of the cone, stabilizer fins or runner cone extensions [6]. Numerical Francis turbine simulation of the flow was performed by Qian et al. [7] in order to investigate the air admission from the spindle hole. Analysis of the draft tube cone air admission showed that the amplitude and the pressure difference in the cross section of the draft tube decreases while the blade frequency pressure pulsation increases in front of the runner. Therefore, proper air discharge to mitigate the pressure pulsations in the draft tube cone of the hydraulic turbine should be chosen according to specific operating conditions. These methods lead to some improvements in reducing the pressure pulsations for a narrow regime but they are not effective or even increase the unwanted effects. Given by the energy injected in the draft tube cone these methods can be divided into active, passive or semipassive control. If an external energy source is used to mitigate or eliminate the vortex rope, the control is called active. Examples of active control include air injection either downstream (through runner cone) or upstream (through wicket gates trailing edge) of the runner [6,8], or tangential water jets at the discharge cone wall [9]. The control involving no additional energy to destroy the vortex rope is called passive. Passive control methods include fins mounted on the cone [10,11], extending cones mounted on the runner's crown [12] or using J-grooves [13].

Resiga et al. [14] proposed a new method in order to mitigate the vortex rope, axial water injected through the runner's crown along to the discharge cone. An experimental test rig was designed and developed in the Hydraulic Machinery Laboratory at "Politehnica" University of Timisoara in order to investigate this new method. The rig is used to determine the parameters of the swirling flow with vortex rope and the optimum water jet in order to mitigate the pressure fluctuations.

[1]Corresponding author.

Contributed by the Fluids Engineering Division of ASME for publication in the JOURNAL OF FLUIDS ENGINEERING. Manuscript received August 10, 2011; final manuscript received June 14, 2012; published online July 30, 2012. Assoc. Editor: Hassan Peerhossaini.

This paper presents our experimental investigations of the swirling flow with vortex rope in order to assess the water injection method benefits. The second section presents the experimental test rig and the swirl apparatus used to generate the swirling flow in a conical diffuser similar to the draft tube cone of a Francis turbine. The third section presents the equipment used for pressure measurements and the results obtained. Pressure data are analyzed to determine the vortex rope amplitude and frequency corresponding to the self-induced instabilities of the decelerated swirling flow. Energetically, the pressure recovery coefficient in the draft tube cone is used to assess the efficiency of this method. The pressure pulsations are analyzed for the swirling flow with vortex rope as well as for the swirling flow with water injection in order to evaluate this method. The last section draws the conclusions.

2 Experimental Test Rig for Swirling Flows

Two different methods are usually employed to generate a swirling flow under the laboratory conditions: using a turbine model or a swirl generator. Using a turbine model is quite expensive. Alternatively, a swirl generator is a simpler solution allowing physical phenomena investigation. For the production of a swirling flow, Kurokawa et al. [13] used an axial flow impeller at about $3.3d$ upstream of the diffuser inlet, where $d(=156\,\text{mm})$ is the inlet pipe diameter. Kurokawa's rig employs an additional blower arranged at far upstream of the divergent channel to widely change the discharge. Another method to generate a swirling flow in a conical diffuser was proposed by Kirschner et al. [15]. The swirl generator is installed instead of the turbine in order to investigate different swirl conditions, and was built with adjustable guide vanes. A straight draft tube was mounted downstream. The cone angle is 2×8.6 deg, similar to the angle of a real draft tube cone.

Based on the large experience accumulated over the decades of design, the hydraulic losses are small in the spiral casing, in the wicket gates, and runner. However, the hydraulic losses still exhibit large variations during the full operating range. According to Vu and Retieb [16] in the case of Francis turbines, the largest fraction of the hydraulic loses is located in the draft tube except in the neighborhood of the best efficiency regime. When the turbine is operated far from the best efficiency point, its losses increase sharply with a corresponding decrease in overall efficiency. This is the reason why researchers focus their efforts to improve the draft tube cone flow.

An experimental test rig was developed to analyze the decelerated swirling flow in a conical diffuser and to evaluate the new water-injection control method. The main purpose of the rig is to reproduce the flow field specific to a conical diffuser with a decelerated swirling flow and the development of the vortex rope. The rig, developed in the Hydraulic Machinery Laboratory at the Politehnica University of Timisoara, is composed of the following main elements: (i) the main hydraulic circuit used to generate the decelerated swirling flow in the conical diffuser; (ii) the auxiliary hydraulic circuit needed to supply water for the jet control method. The main hydraulic circuit (shown in Fig. 1) is employed to generate a flow similar to the one encountered at a partial discharge operated Francis runner while the auxiliary circuit (shown in Fig. 1) is used to inject water in the conical diffuser's inlet through a nozzle.

The swirling flow apparatus is installed along the main hydraulic circuit and it contains two main parts: the swirl generator and the convergent-divergent test section [17]. The swirl generator has an upstream annular section with stationary and rotating blades for generating swirling flow. It has three components: the ogive, the guide vanes, and the free runner. The ogive with four leaned struts has the role to sustain the swirl generator and to deliver the jet water to the nozzle (it can be seen in Fig. 2). The guide vane and the free runner are mounted in the cylindrical section, $D_s = 0.15$ m. The swirl generator was designed to operate similar to a Francis turbine model at partial discharge [18,19]. This part load operating point was chosen at 70% because at this regime the vortex rope is well developed and generates the largest pressure pulsations [20]. The main part of the swirl generator is the free runner. Its main purpose is to redistribute the total pressure at the entrance. The free runner induces an excess of energy near the shroud and a deficit of energy near the hub. Therefore it acts as a turbine at the hub and as a pump at the shroud having a vanishing total torque. The swirl generator's hub and shroud diameters are $D_h = 0.09$ m and $D_s = 0.15$ m, respectively. The 10-bladed runner spins freely and ensures the designed output flow configuration. Teflon bearing was preferred as it ensures low friction. Supplied by the auxiliary hydraulic circuit (Fig. 1(*a*)), the injected water passes through the leaned struts of the ogive, the hub's interior and reaches the nozzle.

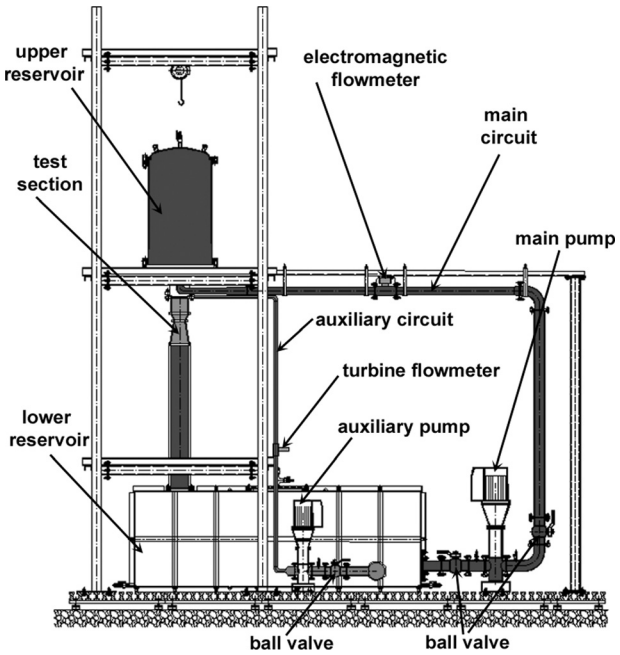

Fig. 1 Experimental closed loop test rig installed in the Hydraulic Machinery Laboratory. Sketch of the test rig with the main elements.

The inverse method [21] was used to design the runner and the guide vanes. The runner's exit velocity profiles resulting from the FLINDT project were imposed for design. These velocity profiles were measured by Ciocan et al. [22] and numerically determined by Stein et al. [23,24]. As a result, the axial and the swirl velocity profiles in the test section are quite similar to the ones measured downstream of the runner of a Francis turbine model according to Fig. 7 from Resiga and Muntean [25]. Note that this is the runaway speed for the swirl generator runner and it is not related to the turbine model runner speed. The dimensionless precession frequency of the vortex rope is expressed using the Strouhal number shown in Table 1. It can be seen that the swirl apparatus generates a vortex rope with Strouhal number equal to 0.39 quite close to the Strouhal number for the model Francis turbine ($\text{Sh} = 0.408$).

The vortex rope visualized in Fig. 3(*a*) was obtained using the above-described swirl. It can be seen that the vortex rope develops along the entire length of the cone. Having a spiral shape with a precession movement, it starts close to the injection nozzle and it disintegrates at the downstream exit having a total length of about 200 mm. When the jet is turned on, it pushes the stagnant region and the associated vortex rope downstream the cone, Fig. 3(*b*) [26].

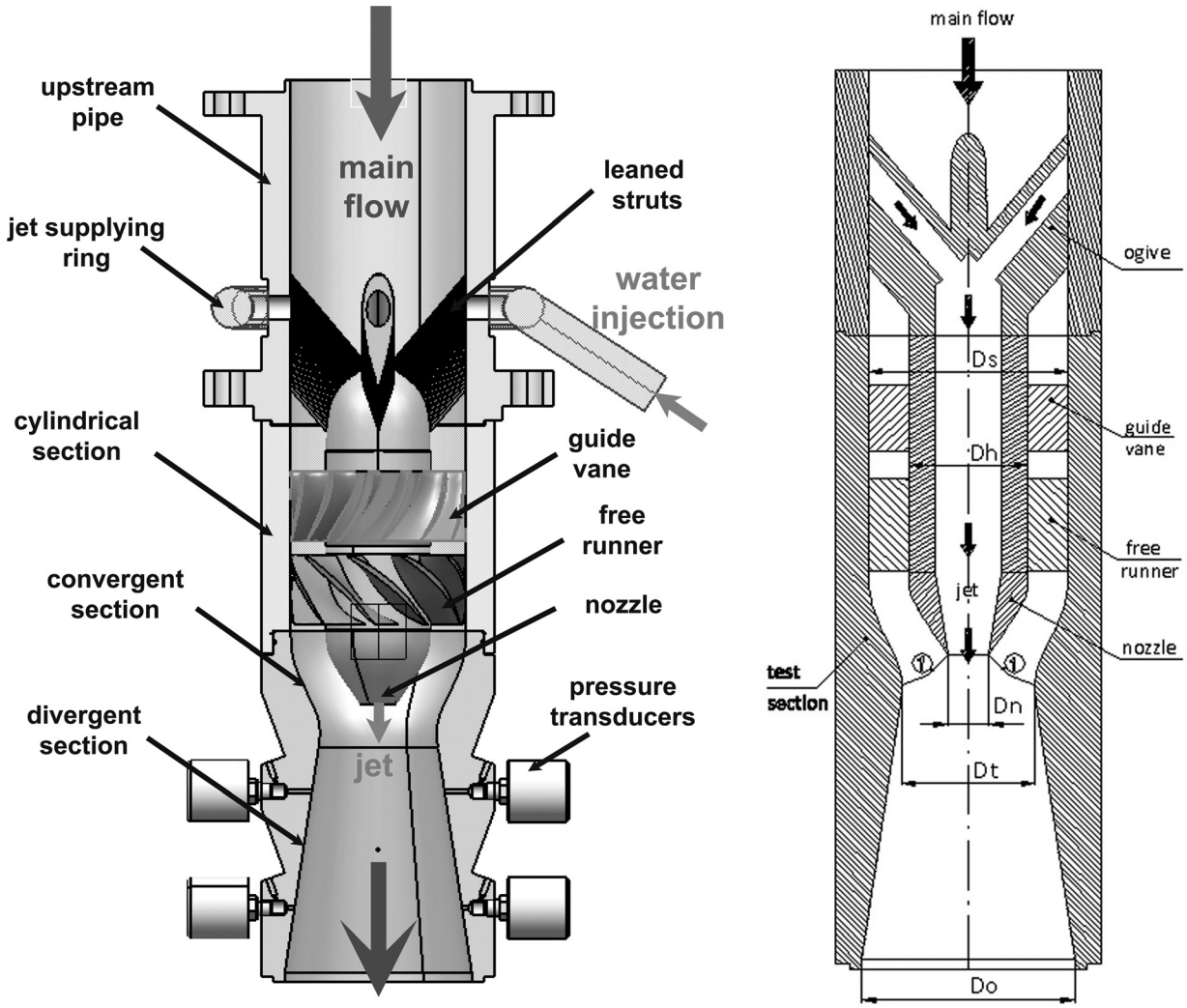

Fig. 2 The swirl apparatus and cross section with the main elements

3 Pressure Measurements

The aim of this research is to assess a new method for diminishing the pressure pulsations and increase pressure recovery in a straight conical diffuser similar to the draft tube cone of a Francis turbine. The recorded unsteady pressure is used to analyze the dynamic and energetic performances. Pressure fluctuation data are used to assess the dynamic behavior while the mean pressure is needed for energetic assessment.

Energetically, the pressure recovery coefficient along the cone is determined by analyzing the averaged pressure. Dynamically, the decelerated swirling flow's amplitude and frequency and the type of conical diffuser's unsteadiness are determined by analyzing the Fourier spectra. The latter is evaluated using two pressure transducers flash mounted on the same level. According to Jacob and Prenat [27], depending on the phase between the two pressure signals the conical diffuser unsteadiness is either rotating or plunging oscillation type.

Table 1 Vortex rope Strouhal number for the model Francis turbine and for the swirl apparatus

	Francis model turbine at partial discharge [22]	Swirl apparatus
f (Hz)	4.17	14.9
D_{ref} (m)	0.4	0.1
V_{ref} (m/s)	4.084	3.82
$Sh = (f \times D_{ref})/V_{ref}$	0.408	0.39

Four levels were selected for pressure measurements as shown in Fig. 4. The top level located in the test section's throat was denoted MG0. This level is considered the benchmark (the references for dimensionless values are being calculated with respect to this level). The other levels MG1, MG2, and MG3 correspond to 50, 100, and 150 mm downstream in the discharge cone, relative to the MG0. The first step of experimental procedure was to confirm that two pressure transducers located on the same level indicate the same static pressure. The capacitive pressure transducers used for measurements have an accuracy of 0.13% within a range of ± 1 bar relative pressure. Having two pressure transducers on the same level, allows the same level average pressure comparison confirming the transducer's accuracy.

The unsteady pressure was measured at the test section's wall to assess the influence of the water injection control method. A main operating discharge of 30 l/s was used for experimental investigation in all regimes. The water jet discharge used for control purposes was calculated as a percentage of the main flow. Pressure pulsation measurements were performed while injecting water of 5%, 7.5%, 9.3%, 10%, 10.9%, 11.3%, 11.6%, 11.9%, 12.5%, 13%, and 14% discharge. The unsteady pressure is measured using eight transducers mounted on the conical diffuser's wall. In order to verify the measurements repeatability ten experiments were performed for each jet discharge value. Each set corresponds to an acquisition time interval of 32 s at a

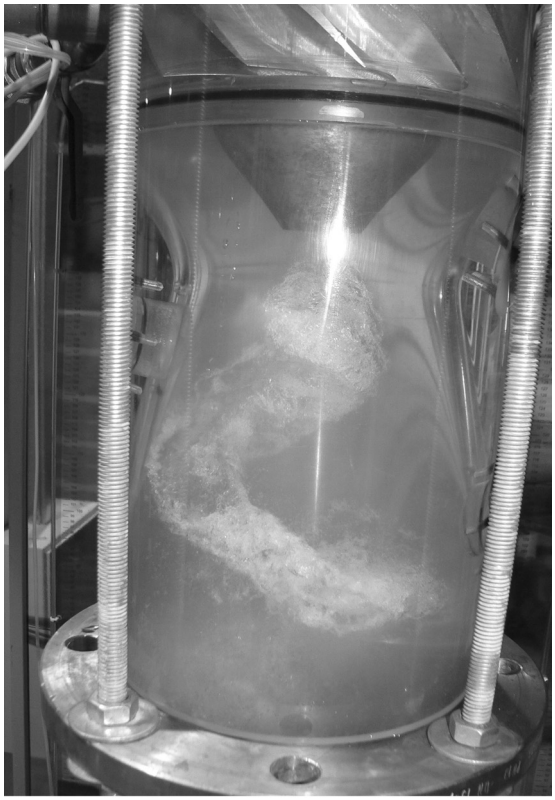

(a)

(b)

Fig. 3 The visualization of the cavitating vortex rope from the discharge cone of the test section (*a*) and with water injection (*b*)

sampling rate of 256 samples/s. The investigations reported in this paper follow two research directions. Energetically, the cone pressure recovery coefficient is evaluated using the experimental data to assess the efficiency of the proposed control method for different jet discharge values. Dynamically, the pressure pulsations are evaluated for several different jet discharge values.

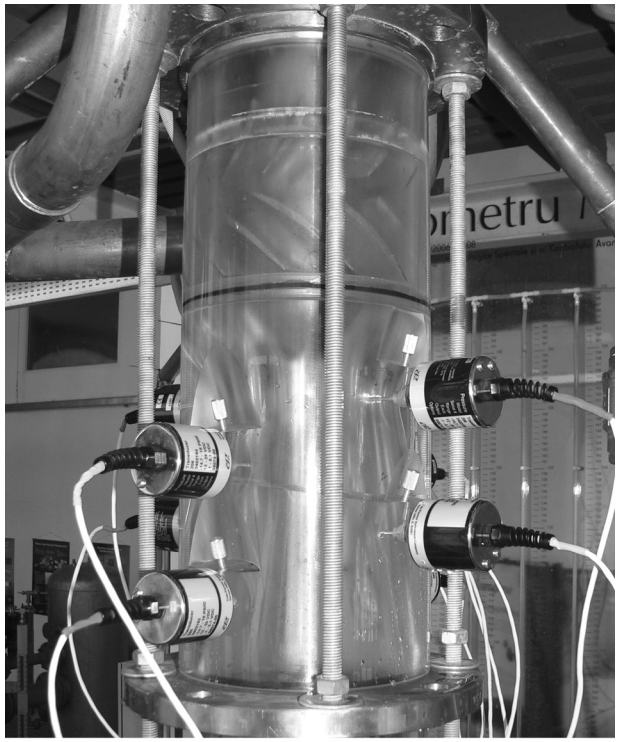

(a)

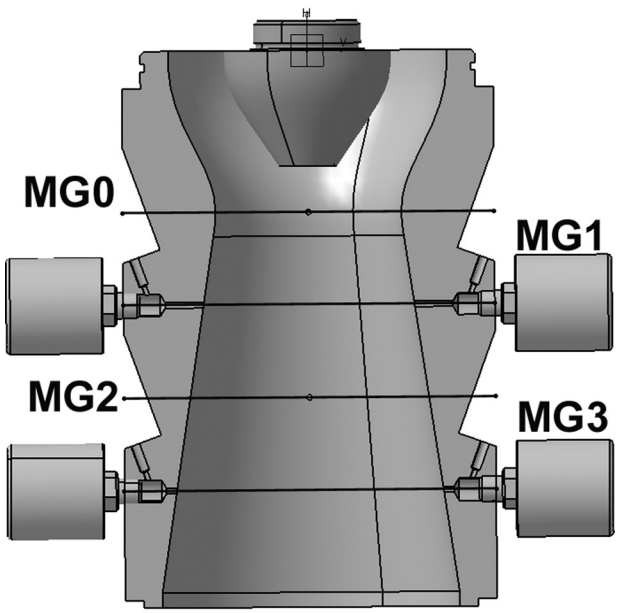

(b)

Fig. 4 The test section with wall flash mounted pressure transducers on the rig (*a*) and the labels for each level (*b*)

4 Pressure Data Analysis

4.1 Averaged Pressure Analysis. Energetically, the mean pressure has to be analyzed for all measurement levels in order to assess the influence of our flow control approach on the overall diffuser efficiency. The pressure recovery coefficient is given by the following equation:

$$c_p = \frac{\overline{p} - \overline{p_{MG0}}}{\rho \cdot v_t^2/2} \tag{1}$$

where c_p is the pressure recovery coefficient, $\overline{p}_{MG0}$ is the mean pressure recorded in the MG0 level, $\overline{p}$ is the mean pressure recorded at downstream levels from MG0 (see Fig. 4), ρ is the water density, and v_t is the throat velocity. The pressure recovery coefficient expressed by Eq. (1) for the MG1, MG2, and MG3 levels in terms of the ratio of Q_{jet}/Q was analyzed. This coefficient (relative to the throat section labeled MG0 which is considered as a reference) is plotted in Fig. 5 for all the above mentioned levels. The measurements have been repeated ten times, with a resulting standard deviation less than 2% as shown with error bars in Fig. 5.

After a drop down at 1%, the pressure recovery coefficient start to increase up to 2% discharge for the first 50 mm along the cone (level MG1), Fig. 5(*a*). At over 2% control jet discharge value, the stagnant region is located below the MG1 level. As such, increasing the control jet discharge over this value causes insignificant pressure recovery coefficient modification at the MG1 level (Fig. 5(*a*)). The pressure recovery coefficient variation related to the control jet discharge at the MG2 level (located in the middle of the cone) reveals two distinctive regions. A significant improvement (about 30%) of the pressure recovery coefficient is observed between 0% and 5% control jet discharge. Over this 5% value, the pressure recovery coefficient increases monotonically up to 60% in the full water injection domain (Fig. 5(*b*)). At the MG3 level one can see a monotonic increase about 30% of the pressure recovery coefficient as the control jet discharge increases from 0% to about 13%, Fig. 5(*c*). It is important to note that the pressure recovery coefficients for levels MG2 and MG3 continue to grow as the control jet discharge exceeds the critical threshold value (11.5%) towards 13%. This suggests a better pressure recovery along the cone up to 13% control jet discharge. However, the optimum control jet discharge value is a balance between the cone recovered energy and the jet hydraulic power [28]. Over the 13% control jet discharge value the pressure recovery coefficient is practically constant for all the levels. Consequently, an analysis of the pressure recovery coefficient variation along the cone is performed for a control jet discharge of 14%. Figure 6 shows a comparison of the pressure recovery coefficient's distribution along the cone in two cases, vortex rope (no control jet) and 14% control jet discharge. One can see an increase of the pressure recovery coefficient for all levels (MG1, MG2, and MG3) in the jet case versus the vortex rope case, Fig. 6. At MG1 level the pressure recovery coefficient increases by 23% (from around 0.55 to around 0.68). The second level MG2 shows a significant improvement of 110% of this coefficient (from around 0.39 to around 0.82). On the third investigated level MG3, one can notice an increase of 47% of this coefficient (from around 0.55 to around 0.81). Figure 6 demonstrates that our control method increases the energy recovery in the cone which exhibits the designed hydrodynamic behavior even in these conditions [17].

4.2 Unsteady Pressure Analysis. Dynamically, the unsteady pressure signal's Fourier spectra has to be analyzed in order to understand the swirling flow configuration and to assess the water injection method. A new approach is employed to analyze the pressure signal. It offers a metric which allows quantitatively dynamical characterization of the unsteady pressure signal. Based on the acquired unsteady pressure signal, this approach leads to an accurate evaluation of the unsteadiness level. Mathematically, it compares two signals having different Fourier spectra (amplitude, harmonics number, and their frequencies). The second signal is reconstructed based on the acquired one using the Parseval's theorem. It has the same frequency as the first harmonic of the acquired signal and root mean square (rms) equivalent amplitude.

The results will be presented as dimensionless. The following reference values are considered in the analysis: (i) the throat diameter of the test section $D_t = 0.1$ m, (ii) the overall throat discharge, which includes the main circuit discharge $Q = 30$ l/s and the jet discharge Q_{jet} (associated with a different water injection regime), (iii) the throat average static pressure denoted $\overline{p}_{MG0}$.

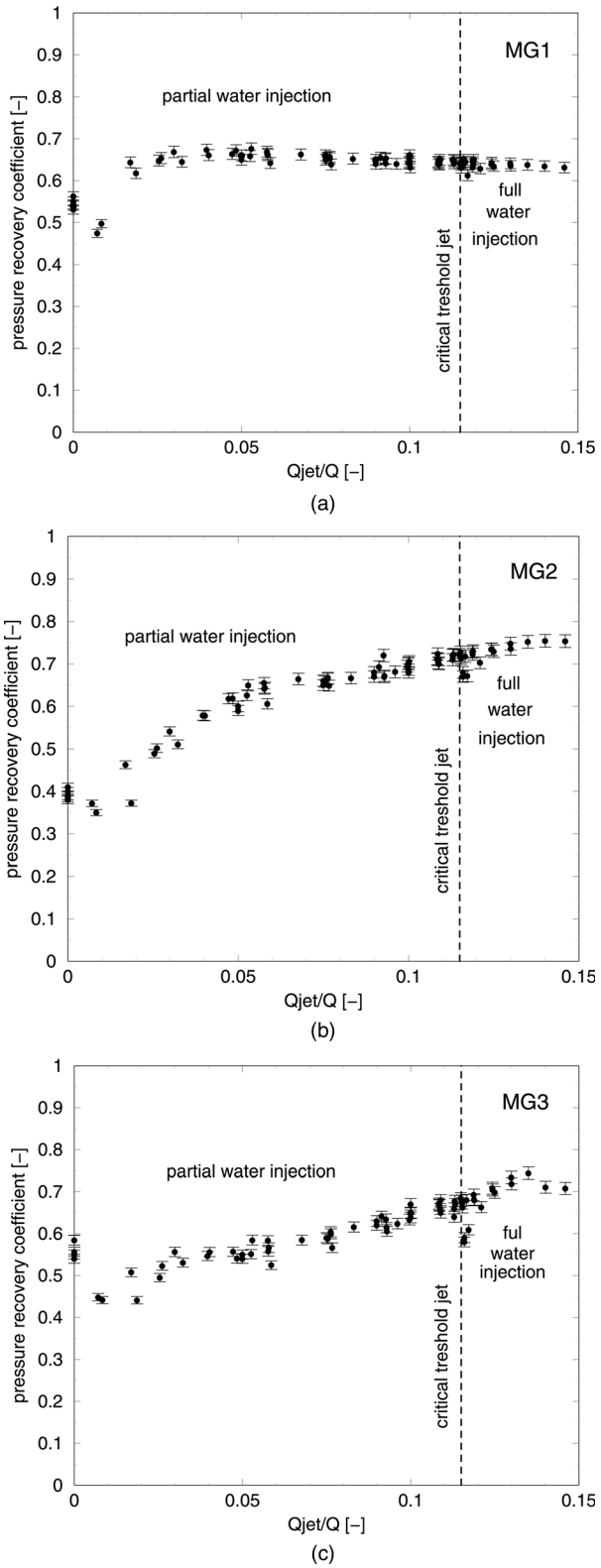

Fig. 5 Evolution of the pressure recovery coefficient for MG1 (*a*), MG2 (*b*), and MG3 (*c*) levels depending on the Q_{jet}/Q

The first dimensionless parameter to be used is the Strouhal number Eq. (2) associated with the frequency. The throat reference velocity value takes into account the overall discharge which includes the main circuit's and the jet's discharges. Particularly, the overall discharge equals to the main circuit's discharge when the jet is turned off,

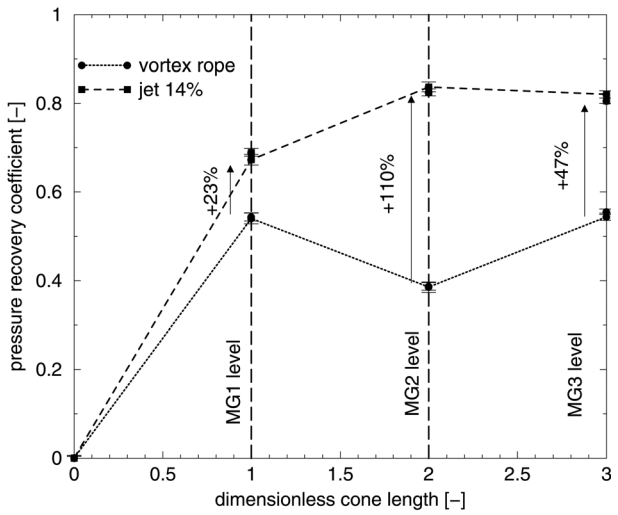

Fig. 6 Pressure recovery coefficient comparison between the swirling flow with vortex rope regime and the full water injection 14% discharge of the main flow at all levels

$$Sh = f \cdot \frac{D_t}{v_t} \quad \text{where} \quad v_t = \frac{4(Q+Q_{\text{jet}})}{\pi D_t^2} \tag{2}$$

The second dimensionless parameter to be used is the pressure's amplitude. This is described in the following. The Fourier transform for a continuous signal $p(t)$ is defined according to statistical theory [29,30]

$$p(t) = \frac{p_0}{2} + \sum_{m=1}^{\infty}\left[a_m \cos\left(\frac{2\pi mt}{T}\right) + b_m \sin\left(\frac{2\pi mt}{T}\right)\right] \tag{3}$$

where T is the period, m the mode, t the time, and a_m and b_m are the Fourier transform coefficients defined as

$$a_m = \frac{2}{T}\int_{t_0}^{t_0+T} p(t)\cos\left(\frac{2\pi mt}{T}\right)dt; \quad b_m = \frac{2}{T}\int_{t_0}^{t_0+T} p(t)\sin\left(\frac{2\pi mt}{T}\right)dt \tag{4}$$

with t_0 being the initial time.

The first coefficient represents the average value $\bar{p}$ of the signal and it is defined in Eq. (5),

$$p_0 = \frac{2}{T}\int_{t_0}^{t_0+T} p(t)dt = 2\bar{p} \tag{5}$$

where $p_0/2$ is the mean value of $p(t)$. The amplitude and the angular frequency can be written as follows:

$$A_m = \sqrt{a_m^2 + b_m^2}; \quad \omega_m = m\frac{2\pi}{T} \tag{6}$$

The Parseval's theorem applied to the Fourier transform is written as below,

$$\frac{1}{T}\int_{t_0}^{t_0+T} |p(t)|^2 dt = \left(\frac{1}{2}p_0\right)^2 + \frac{1}{2}\sum_{m=1}^{\infty}\left(a_m^2 + b_m^2\right) \tag{7}$$

The pressure root mean square (rms) is defined according to the following equation:

$$p_{\text{rms}} = \sqrt{\frac{1}{T}\int_{t_0}^{t_0+T} (p(t)-\bar{p})^2 dt} \tag{8}$$

Appling the Parseval's theorem yields

$$p_{\text{rms}}^2 = \frac{1}{T}\int_{t_0}^{t_0+T} p^2(t)dt - \bar{p}^2 \tag{9}$$

According to this theorem, the pressure's rms is defined as

$$p_{\text{rms}}^2 = \frac{1}{2}\sum_{m=1}^{\infty}\left(a_m^2 + b_m^2\right) \tag{10}$$

For a discrete signal the following equation applies:

$$p_{\text{rms}} = \sqrt{\frac{1}{N}\sum_{i=1}^{N}(p_i - \bar{p})^2} = \sqrt{\frac{1}{2}\sum_{m} A_m^2} \tag{11}$$

The amplitude's dimensionless form for a discrete signal can be defined as

$$A = \sqrt{2}p_{\text{rms}}$$

leading to

$$\bar{A} = \left(\sqrt{2}p_{\text{rms}}\right)\Big/\left(\frac{1}{2}\rho v_t^2\right) \quad \text{where} \quad v_t = \frac{4(Q+Q_{\text{jet}})}{\pi D_t^2} \tag{12}$$

This means that the equivalent amplitude (A) of the pressure pulsation is proportional to the rms. In other words, the equivalent amplitude collects all spectrum contributions. As a result, the original signal can be accurately reconstructed using its fundamental frequency and the equivalent amplitude computed based on the pressure signal. Both the acquired (points) and the reconstructed signals according to the above approach (continuous line), can be seen in Fig. 7 for all investigated levels. However, this procedure may be employed to reconstruct rms equivalent signals using the fundamental frequency and a number of harmonics. With no control water jet the swirling flow loses the stability and develops the vortex rope and associated unsteadiness. Consequently, the vortex rope's Strouhal number is 0.39 as shown in Fig. 8(*b*). A qualitative model of the vortex rope flow field was given by Nishi et al. [31] who observed a quasi-stagnant (stalled) central region with the spiral vortex core wrapped around it. This statement was validated with experimental data using the FLINDT turbine model operating at part load by Resiga et al. [32]. The vortex rope geometrical shape is almost cylindrical having a very small eccentricity (see Fig. 3) close to the nozzle. It is important to note that at MG0 and MG1 levels (Fig. 7), the amplitude of the fundamental frequency associated with the vortex rope is dominant, while the higher harmonics have negligible amplitudes. The highest equivalent amplitude corresponds to the MG2 level, Fig. 8(*a*) (the rhombus-marked curve). These differences in amplitude for each level (Fig. 8(*a*), corresponding to $Q_{\text{jet}}/Q = 0$) are due to the vortex rope shape. Indeed, the angle of the cone the vortex rope wraps on larger than the geometry cone's angle. As a result, the vortex rope's eccentricity is largest at the MG2 level. As it advances downstream, the vortex rope loses strength and begins to disintegrate (level MG3) and its higher harmonics increase significantly [33,34].

When starting to inject the water, the stagnant region associated with the vortex rope is gradually pushed downstream of the cone. Consequently, at 5% control jet discharge the vortex rope's amplitudes remain almost constant for the MG0 level, decrease for the next two levels (MG1 and MG2) approximately by 10%, and increase for the last level (MG3) by approximately 40% (Fig. 8(*a*)). The vortex rope Strouhal number sharply decreases from 0.39 to 0.27 (Fig. 8(*b*)). Exceeding this discharge value leads to a monotonous decrease of frequency and amplitudes for all

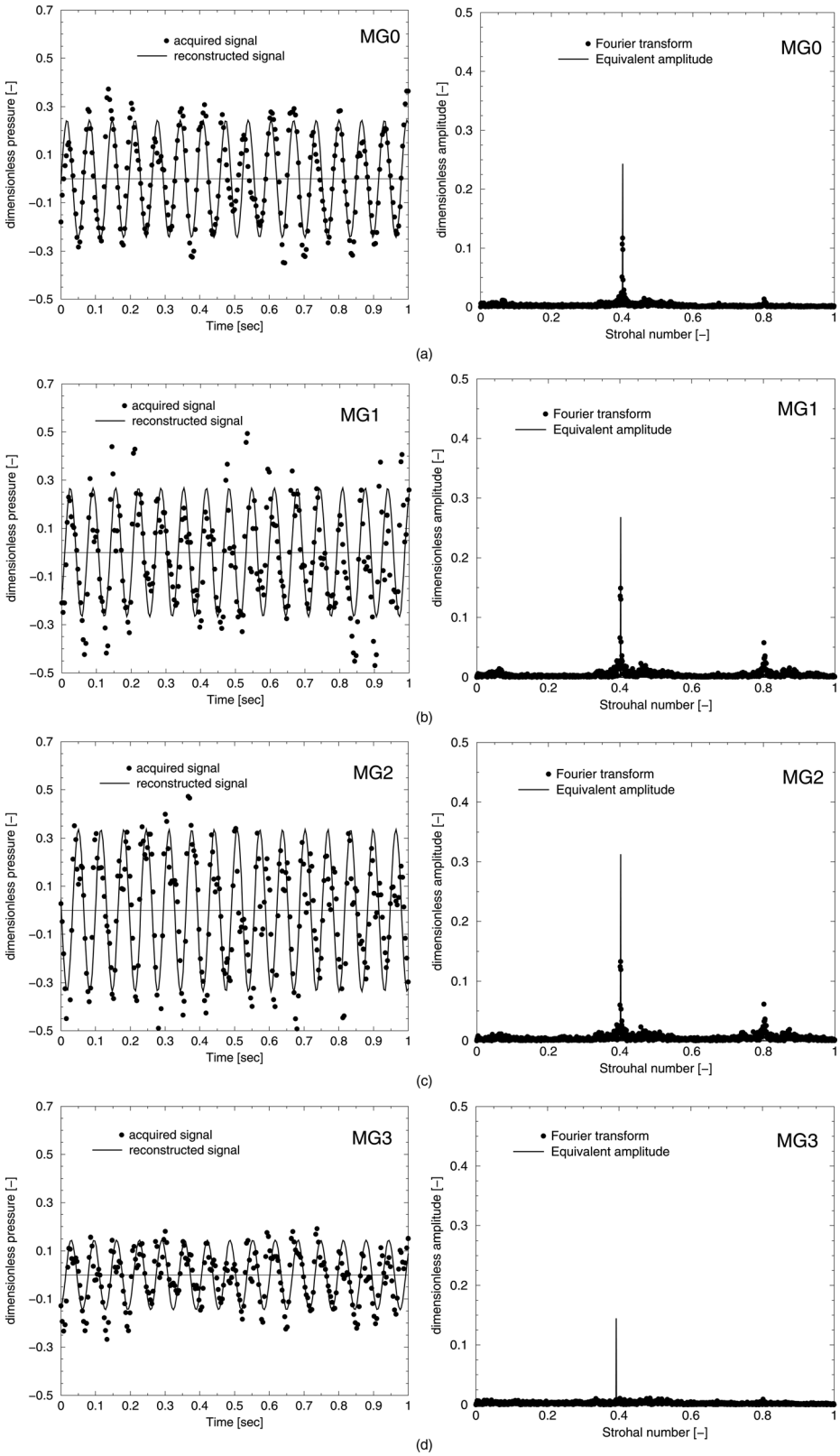

Fig. 7 Reconstructed signal against acquired signal for MG0, MG1, MG2, and MG3 levels (left) and equivalent amplitude overlapped with Fourier spectra of pressure signal (right) in the case of swirling flow with vortex rope

levels until reaching the 11.5% jet discharge critical threshold. At 11.5% jet discharge, the frequency decreases by 35% with respect to no control jet. Correspondingly, the amplitudes decrease for all levels except MG3 due to the fact that the top of the stagnant region reaches this level. Over this critical threshold, this region gets completely pushed out of the cone. As a result, a sudden drop is noted in both amplitudes (at all levels) and frequency. Further jet discharge increase causes no modification in amplitudes and

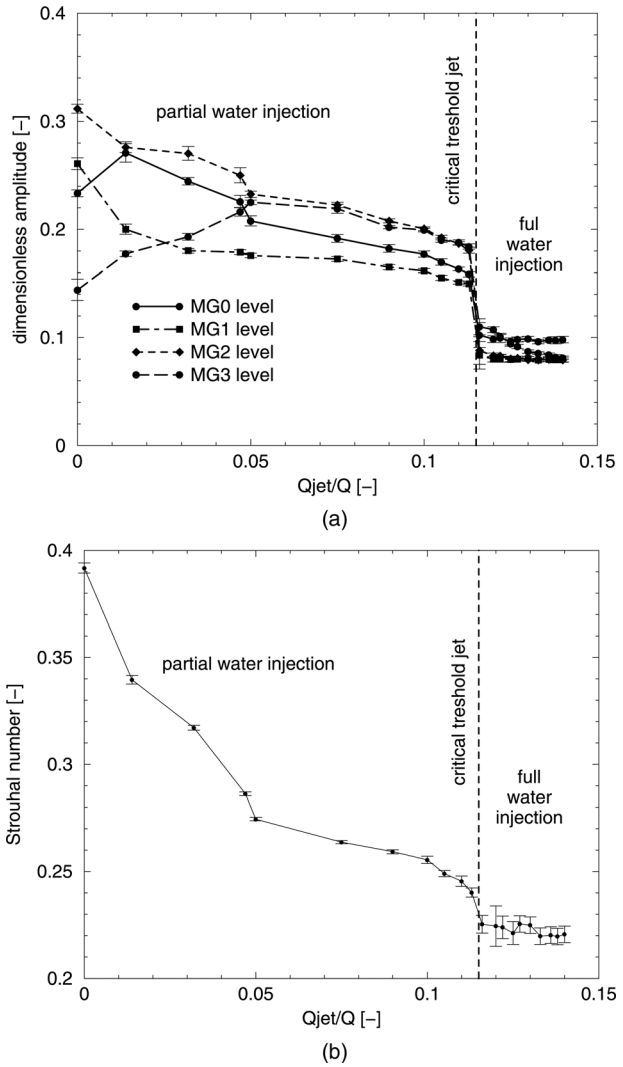

Fig. 8 Equivalent amplitudes corresponding to levels from the test section (*a*) and Strouhal number (*b*) versus ratio Q_{jet}/Q

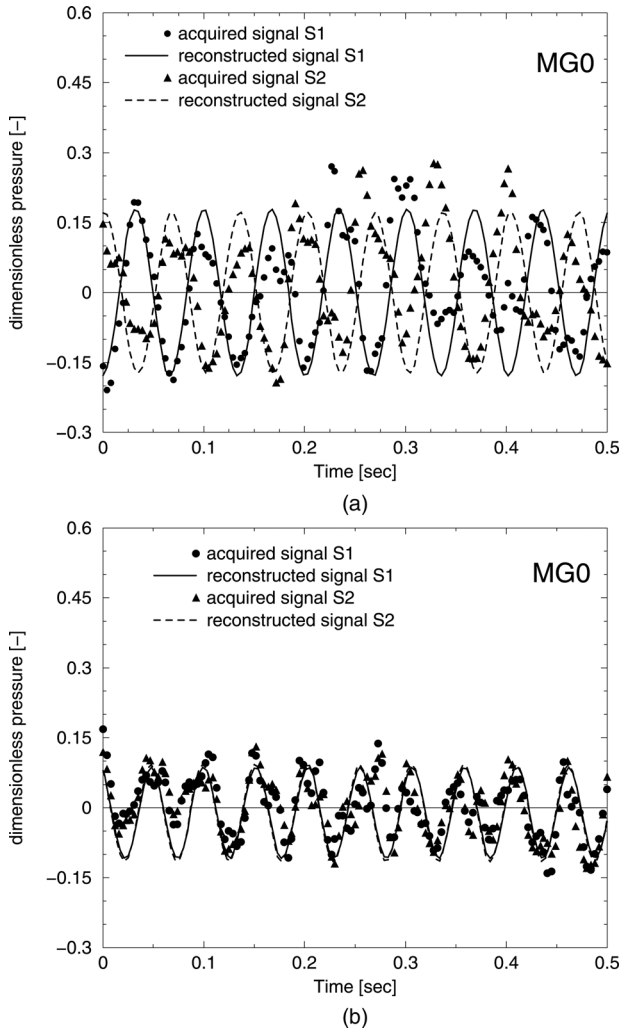

Fig. 9 Dimensionless pressure signals for MG0 level for swirling flow with vortex rope (*a*) and 14% full water injection (*b*)

frequency. Both plots in Fig. 8 include the 2% error band of the main value for each measuring point. It is important to note that below the critical jet threshold the error bands are small. This occurs due to the fact that the value of the amplitudes and frequency associated to the swirling flow are significantly larger than the noise. Over the threshold, the error bands increase due to the fact that the noise becomes significant with respect to the measured values.

4.3 Pressure Signal Decomposition. As mentioned above, according to Jacob and Prenat [27], there are two types of draft tube cone pulsations. The plunging type (synchronous) is acting like a water hammer along the cone axis. The rotation type (asynchronous) is acting in the cross sections. A minimum of two sensors located on the same section are required for measurements in order to evaluate this pulsation type. The asynchronous pulsation is produced by instabilities, such as the vortex rope due to its shape and its precession motion, Koutnik et al. [35]. Two unsteady pressure signals S1 and S2 are used to discriminate between the two pulsation types as follows:

$$\frac{S_1+S_2}{2} \Rightarrow \text{Synchronous component (plunging) of the pressure signal} \tag{13}$$

$$\frac{S_1-S_2}{2} \Rightarrow \text{Asynchronous component (rotating) of the pressure signal} \tag{14}$$

In this analysis, the S1 and S2 signals are reconstructed from the acquired experimental data using the procedure based on the Parceval's theorem. As described above, this procedure was employed at all levels for ten cases (from no jet to 14% control jet discharge). Figure 9 exemplifies the S1 and S2 reconstructed signals in the two outermost cases for the MG0 level: no control jet and 14% control jet discharge.

As mentioned above, each reconstructed signal has the same frequency as the first harmonic of the acquired signal used and its amplitude is rms-equivalent. Therefore, the reconstructed signal is sinusoidal. The phase between the two reconstructed signals indicates the type of pressure pulsation. Indeed, if S1 and S2 are in phase then according to Eq. (14) the asynchronous component vanishes. In this first ideal case, only the pure plunging pulsation is detected. On the contrary, when S1 and S2 are out of phase, according to Eq. (13) the synchronous component vanishes. This is the second ideal case in which only the pure rotation component is found. Generally, both pulsation types are expected to be found in all investigated cases. The pressure pulsation type's distributions along the cone in the two outermost cases are displayed in Fig. 10. The swirling flow with vortex rope case (Fig. 10(*a*)) reveals predominant rotational pressure pulsations at all

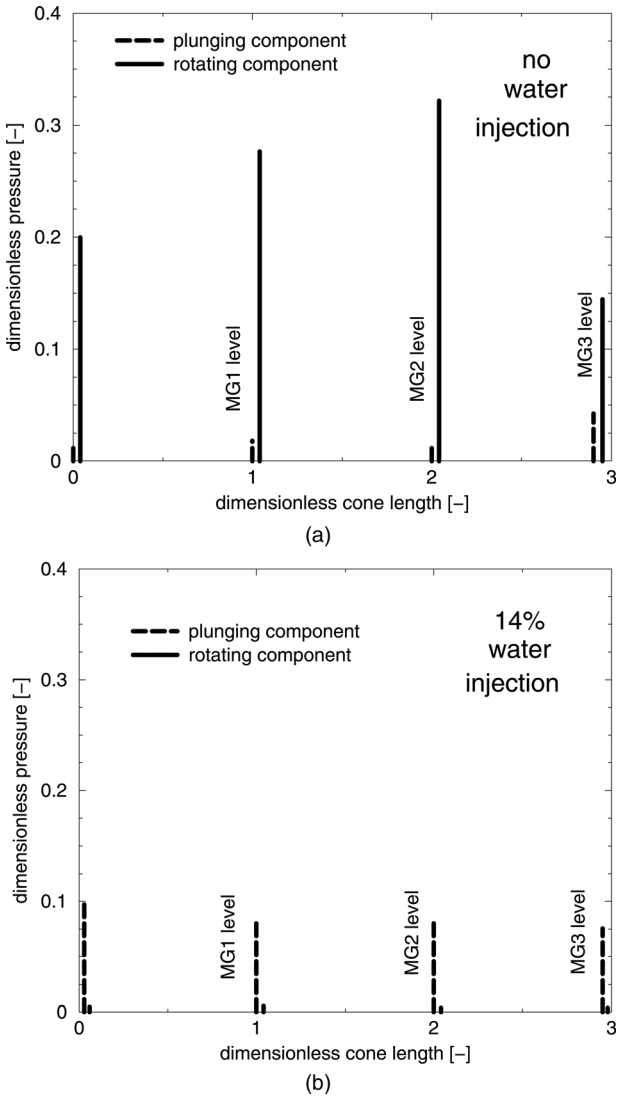

Fig. 10 Dimensionless pressure signal decomposition for swirling flow with vortex rope (*a*) and 14% water injection (*b*) in the length of the cone

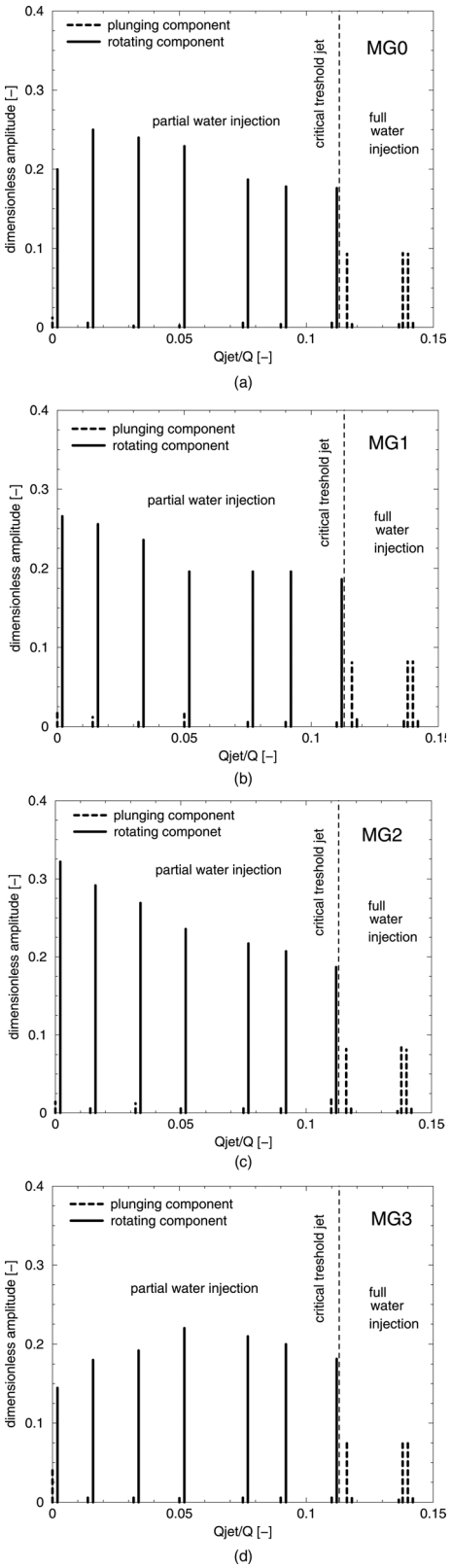

Fig. 11 Pressure pulsations types' distributions versus control jet discharge

investigated levels. This is expected due to the vortex rope precession motion. On the contrary, the 14% control jet discharge (Fig. 10(*b*)) highlights a significant decrease (about 30 times for the most significant level – MG2) of the rotational pulsation component. However, one can observe an increase (about five times for the MG2 level) of the plunging component of the pressure pulsation in comparison to the vortex rope case. We conclude from Fig. 10 that the jet injection along the cone axis removes the precessing helical vortex and its associated rotating pressure fluctuations. As a result, the swirling flow becomes axisymmetric, and the relative increase in the level of plunging pressure fluctuations might be related to a possible "subcritical" swirl configuration, as defined by Benjamin [36], when the swirling flow can sustain axisymmetric waves.

Figure 11 displays the two pressure component types (plunging and rotational) distribution with respect to the control jet discharge values for the four investigated levels. The following ten values of jet discharges were used for measurements: 0%, 1.4%, 3.2%, 5%, 7.5%, 9%, 11%, 11.6%, 13.8%, and 14%. The rotational component of the pressure pulsation associated with the vortex rope is significant for all jet values located in the partial water injection domain. In the full water injection domain, the plunging pulsation becomes predominant for all injection values. This behavior characterizes all investigated levels in Fig. 11. Overall, the pulsations have decreased. The significant decrease of the rotational pulsation component allows a safe turbine operation at these conditions.

5 Conclusions

The paper investigates the decelerated swirling flow with vortex rope in a conical diffuser, using a swirl generator that mimics the flow in the discharge cone of hydraulic turbines operated at partial discharge. A novel flow control technique which uses axial injection is proposed, in order to improve the pressure recovery coefficient and to mitigate the pressure pulsations. The unsteady pressure measurements were performed on the wall test sections. Eight points located on four levels were investigated. For each operating mode (swirling flow with vortex rope or swirling flow with water injection) ten sets were measured.

Firstly, the average pressure was determined to compute the pressure recovery coefficient in order to assess the energetic performance of the new control method. The jet discharge increase reveals two domains: the partial water injection and the full water injection. The two domains are separated by the critical water injection threshold at 11.5% discharge. The experiments reveal an increase of the pressure recovery coefficient when increasing the control jet discharge. Overall, the pressure recovery coefficient associated with the full water injection leads to about 30% improvements. The highest improvement was measured for the MG2 level (located in the middle of the cone) and it was about 60%. This fact suggests a better energetic behavior of compact discharge cones. These overall results demonstrate an improved energetic cone behavior at this operating point. However, the optimum control jet discharge value has to be selected as a balance between the draft tube cone recovered energy and the jet hydraulic power. Although, the method proves consistent energy recovery, the 11.5% jet discharge value is prohibitive from an energetic point of view if taking into account that the control jet is considered a volumetric loss.

Secondly, the dynamical behavior associated to this control method was investigated by analyzing the pressure signal's Fourier spectra. A new method based on the Parceval's theorem was employed to reconstruct the acquired unsteady pressure signal. The result of this procedure was a sinusoidal signal having the same frequency as the first harmonic of the acquired signal and rms equivalent amplitude. As the control jet discharge increases, the unsteady pressure frequency decreases monotonically in the partial water injection domain. During the full water injection domain, the frequency remains practically constant. Generally, the unsteady pressure amplitudes decrease as the jet discharge increases in the partial water injection domain (MG0 and MG3 show a different variation pattern for small discharge values). The amplitudes variations display a sudden drop at 11.5% jet discharge. This is the reason why the 11.5% discharge was labeled "critical threshold jet." Above this value, the amplitudes exhibit negligible variations with regard to the jet discharge. Therefore, the instabilities associated with the vortex rope have been mitigated. As such this domain becomes desirable for operation.

The unsteady pressure signal is decomposed into rotational and plunging components. The rotational component of pressure pulsation associated with the vortex rope is significant for all jet values located in the partial water injection domain. In the full water injection domain, the plunging pulsation becomes dominant for all injection values, but with small amplitudes. In general, the pulsations have decreased. The significant decrease of the rotational pulsation component suggests operation under these conditions. However, the plunging pulsation propagates into the whole hydraulic system. Mitigation of this component is the subject of future research.

Generally, the proposed control method leads to an improvement of energetic and dynamic performances of the decelerated swirling flow in the discharge cone. The necessary jet discharge values to attain optimum operation conditions have to be evaluated particularly from case to case. Each case will be defined by the cone geometry and the swirling flow configuration. Although 0.115 jet discharge seems to be too large for a real turbine with respect to pumping energy, one should note that the jet does not necessarily need a separate water supply. The novel flow-feedback technique proposed by Susan-Resiga et al. [25] uses a fraction of the main discharge, collected near the wall, at the cone outlet, to supply the jet. It is proved numerically [25] and experimentally [37] that the pressure excess at the cone wall with respect to nozzle outlet can drive the control jet with large enough discharge in order to mitigate the central stagnation region and associated vortex rope.

Acknowledgment

This research was supported by the CNCSIS - UEFISCSU, Exploratory Research Project No. PN II -IDEI code 799/2008.

Nomenclature

a_m, b_m(Pa) = Fourier transform coefficients
D_h(m) = hub diameter of the swirl generator, $D_h = 0.09$(m)
D_i(m) = nozzle exit diameter, $D_i = 0.033$(m)
D_o(m) = outlet diameter from the test section, $D_o = 0.16$(m)
D_s(m) = shroud diameter of the swirl generator, $D_s = 0.15$(m)
D_t(m) = reference diameter from the throat of the convergent-divergent test section, $D_t = 0.1$(m)
f(Hz) = dominant frequency from Fourier spectrum
$Q(\mathrm{m}^3/\mathrm{s})$ = main discharge from the primary hydraulic circuit
$Q_{\mathrm{jet}}(\mathrm{m}^3/\mathrm{s})$ = jet discharge at the nozzle
c_p = pressure recovery coefficient
$p(t)$ = continuous pressure signal
$\overline{p}$(Pa) = average pressure for each level
p_0(Pa) = mean value of a pressure signal
$\overline{p}_{\mathrm{MG0}}$(Pa) = average pressure from level MG0 situated in the throat of convergent-divergent test section
p_{rms}(Pa) = root mean square of a continuous pressure signal
Sh = Strouhal number
S_1, S_2 = pressure signals measured for the same level
v_t(m/s) = reference velocity from the throat of convergent-divergent test section

References

[1] Susan-Resiga, R., Ciocan, G. D., Anton, I., and Avellan, F., 2006, "Analysis of the Swirling Flow Downstream a Francis Turbine Runner," ASME J. Fluids Eng., **128**, pp. 177–189.
[2] Rheigans, W. J., 1940, "Power Swings in Hydroelectric Power Plant," Trans. ASME, **62**(174), pp. 171–184.
[3] Wang, F., Li, X., and Ma, J. Y. M., 2009, "Experimental Investigation of Characteristic Frequency in Unsteady Hydraulic Behavior of a Large Hydraulic Turbine," J. Hydrodynam., **21**(1), pp. 12–19.
[4] Baya, A., Muntean, S., Câmpian, V. C., Cuzmoş, A., Diaconescu, M., and Bălan, G., 2010, "Experimental Investigations of the Unsteady Flow in a Francis Turbine Draft Tube Cone," Proceedings of the 25th IAHR Symposium on Hydraulic Machinery and Systems, IOP Conf. Ser.: Earth and Environmental Science of Institute of Physics, **12**, p. 012007.
[5] Arpe, J., Nicolet, C., and Avellan, F., 2009, "Experimental Evidence of Hydroacoustic Pressure Waves in a Francis Turbine Elbow Draft Tube for Low Discharge Conditions," ASME J. Fluids Eng., **131**(8), p. 081102.
[6] Thicke, R. H., 1981, "Practical Solutions for Draft Tube Instability," Int. Water Power Dam Constr., **33**(2), pp. 31–37.
[7] Qian, Z.-D., Yang, J.-D., and Huai, W.-X., 2007, "Numerical Simulation and Analysis of Pressure Pulsation in Francis Hydraulic Turbine With Air Admission," J. Hydrodynam., **19**(4), pp. 467–472.
[8] Pappilon, B., Sabourin, M., Couston, M., and Deschenes, C., 2002, "Methods for Air Admission in Hydro Turbines," Proceedings of the 21st IAHR Symposium on Hydraulic Machinery and Systems, Lausanne, Switzerland, pp. 1–6.
[9] Kjeldsen, M., Olsen, K., Nielsen, T., and Dahlhaug, O., 2006, "Water Injection for the Mitigation of Draft Tube Pressure Pulsations," IAHR International Meeting of the Workgroup on Cavitation and Dynamic Problems in Hydraulic Machinery and Systems, Barcelona, Spain.
[10] Nishi, M., Wang, X. M., Yoshida, K., Takahashi, T., and Tsukamoto, T., 1996, "An Experimental Study on Fins, Their Role in Control of the Draft Tube Surging," *Hydraulic Machinery and Cavitation*, E. Cabrera, V. Espert, and F. Martínez, eds., Kluwer Academic Publishers, Dordrecht, The Netherlands, pp. 905–914.
[11] Miyagawa, K., Sano, T., Kunimatsu, N., Aki, T., and Nishi, M., 2006, "Flow Instability With Auxiliary Parts in High Head Pump – Turbines," Proceedings of the 23rd IAHR Symposium on Hydraulic Machinery and Systems, Yokohama, Japan, Paper No. F307.

[12] Vevke, T., 2004, "An Experimental Investigation of Draft Tube Flow," Ph.D. thesis, Norwegian University of Science and Technology, Trondheim, Norway.
[13] Kurokawa, J., Kajigaya, A., Matusi, J., and Imamura, H., 2000, "Suppression of Swirl in a Conical Diffuser by Use of J-Groove," Proceedings of the 20th IAHR Symposium on Hydraulic Machinery and Systems, Charlotte, NC, Paper No. DY-01.
[14] Susan-Resiga, R., Vu, T. C., Muntean, S., Ciocan, G. D., and Nennemann, B., 2006, "Jet Control of the Draft Tube in Francis Turbines at Partial Discharge," Proceedings of the 23rd IAHR Symposium on Hydraulic Machinery and Systems, Yokohama, Japan, Paper No. F192.
[15] Kirschner, O., Grupp, J., and Schmidt, H., 2008, "Experimental Investigation of Vortex Control in a Simplified Straight Draft Tube Model," 4th German-Romanian Workshop of Vortex Dynamics in Hydraulic Machinery, Stuttgart, Germany, IHS, University of Stuttgart.
[16] Vu, T. C., and Retieb, S., 2002, "Accuracy Assessment of Current CFD Tools to Predict Hydraulic Turbine Efficiency Hill Chart," Proceedings of the 21st IAHR Symposium on Hydraulic Machinery and Systems, Lausanne, Switzerland, pp. 193–198.
[17] Bosioc, A., Susan-Resiga, R., and Muntean, S., 2008, "Design and Manufacturing of a Convergent-Divergent Section for Swirling Flow Apparatus," 4th German-Romanian Workshop in Turbomachinery, Stuttgart, Germany, IHS, University of Stuttgart.
[18] Avellan, F., 2000, "Flow Investigation in a Francis Draft Tube: The FLINDT Project," Proceedings of the 20th IAHR Symposium on Hydraulic Machinery and Systems, Charlotte, NC, Paper No. DY-03.
[19] Susan-Resiga, R., Muntean, S., Tanasa, C., and Bosioc, A. I., 2008, "Hydrodynamic Design and Analysis of a Swirling Flow Generator," 4th German-Romanian Workshop of Vortex Dynamics in Hydraulic Machinery, Stuttgart, Germany, IHS, University of Stuttgart.
[20] Bosioc, A., Tanasa, C., Muntean, S., and Susan-Resiga, R., 2010, "Pressure Recovery Improvement in a Conical Diffuser With Swirling Flow and Jet Injection," Proc. Rom. Acad., Ser. A, **11**(3), pp. 245–252.
[21] Zangeneh, M., 1991, "A Compressible Three-Dimensional Design Method for Radial and Mixed Flow Turbomachinery Blades," Int. J. Numer. Methods Fluids, **13**, pp. 599–624.
[22] Ciocan, G., Iliescu, M., Vu, T. C., Nennemann, B., and Avellan, F., 2007, "Experimental Study and Numerical Simulation of the FLINDT Draft Tube Rotating Vortex," ASME J. Fluids Eng., **129**, pp. 146–158.
[23] Stein, P., Sick, M., Doerfler, P., White, P., and Braune, A., 2006, "Numerical Simulation of the Cavitating Draft Tube Vortex in a Francis Turbine," Proceedings of the 23rd IAHR Symposium on Hydraulic Machinery and Systems, Yokohama, Japan, p. 228.
[24] Stein, P., 2007, "Numerical Simulation and Investigation of Draft Tube Vortex Flow," Ph.D. thesis, Coventry University, United Kingdom.
[25] Susan-Resiga, R., and Muntean, S., 2008, "Decelerated Swirling Flow Control in the Discharge Cone of Francis Turbines," The 4th International Symposium on Fluid Machinery and Fluid Engineering, J. Xu, Y. Wu, and Y. Zhang, eds., Beijing, China, Springer, pp. 89–96.
[26] Bosioc, A., Tanasa, C., Muntean, S., and Susan-Resiga, R., 2009, "2D LDV measurements of Swirling Flow in a Simplified Draft Tube," The 14th International Conference on Fluid Flow Technologies, Budapest, Hungary.
[27] Jacob, T., and Prenat, J., 1996, "Francis Turbine Surge: Discussion and Data Base," Proceedings of the 18th IAHR Symposium on Hydraulic Machinery and Cavitation, Valencia, Spain, Vol. 2, pp. 855–865.
[28] Susan-Resiga, R., Muntean, S., Hasmatuchi, V., Anton, I., and Avellan, F., 2010, "Analysis and Prevention of Vortex Breakdown in the Simplified Discharge Cone of a Francis Turbine," ASME J. Fluids Eng., **132**(5), p. 051102.
[29] Mandel, J., 1964, *The Statistical Analysis of Experimental Data*, Dover Publications, Inc., New York.
[30] Riley, K. F., Hobson, M. P., and Bence, S. J., 2002, "Mathematical Methods for Physics and Engineering," Cambridge University Press, Cambridge, United Kingdom.
[31] Nishi, M., Matsunaga, S., Okamoto, M., Uno, M., and Nishitani, K., 1988, "Measurements of Three-Dimensional Periodic Flow in a Conical Draft Tube at Surging Condition," Flows in Non Rotating Turbomachinery Components, FED, **69**, pp. 81–88.
[32] Susan-Resiga, R., Muntean, S., Stein, P., and Avellan, F., 2009, "Axisymmetric Swirling Flow Simulation of the Draft Tube Vortex in Francis Turbines at Partial Discharge," Int. J. Fluid Mach. Syst., **2**(4), pp. 295–302.
[33] Muntean, S., Susan-Resiga, R. F., and Bosioc, A. I., 2009, "3D Numerical Analysis of Unsteady Pressure Fluctuations in a Swirling Flow Without and With Axial Water Jet Control," Proceedings of the 14th International Conference on Fluid Flow Technologies (CMFF'09), Budapest, Hungary, Vol. 2, pp. 510–518.
[34] Zhang, R., Mao, F., Wu, J., Chen, S., Wu, Y., and Liu, S., 2009, "Characteristics and Control of the Draft-Tube in Part-Load Francis Turbine," ASME J. Fluids Eng., **131**(2), p. 021101.
[35] Koutnik, J., Krüger, K., Pochyly, F., Rudolf, P., and Haban, V., 2006, "On Cavitating Vortex Rope Form Stability During Francis Turbine Part Load Operation," IAHR International Meeting of the Workgroup on Cavitation and Dynamic Problems in Hydraulic Machinery and Systems, Barcelona, Spain.
[36] Benjamin, T., 1962, "Theory of Vortex Breakdown Phenomenon," J. Fluid Mech., **14**, pp. 593–629.
[37] Tanasa, C., Bosioc, A. I., Muntean, S., and Susan-Resiga, R., 2011, "Flow-Feedback Control Technique for Vortex Rope Mitigation From Conical Diffuser of Hydraulic Turbines," Proc. Rom. Acad., Ser. A, **12**(2), pp. 125–132.